Comparison of sample preparation techniques for the ESI-FT-ICR-MS analysis of humic and fulvic acids

Aleksandar I. Goranov[1,#], Amanda M. Tadini[1,2#], Ladislau Martin-Neto[2], Alberto C. C. Bernardi[3], Patricia P. A. Oliveira[3], José R. M. Pezzopane[3], Débora M.B.P.Milori[2], Stéphane Mounier[4], Patrick G. Hatcher[1,*]

1. Department of Chemistry and Biochemistry, Old Dominion University, Norfolk, VA, USA
2. Brazilian Agricultural Research Corporation, Embrapa Instrumentation, São Carlos, SP, Brazil
3. Brazilian Agricultural Research Corporation, Embrapa Southeast Livestock, São Carlos, SP, Brazil
4. University of Toulon, Aix Marseille University, CNRS/INSU, IRD, MIO, Mediterranean Institute of Oceanography, Toulon, France

[#]Authors contributed equally to this work.

*Corresponding author e-mail: Dr. Patrick G. Hatcher (phatcher@odu.edu)

Table of Contents

Section 1. Sampling sites.....2
Section 2. Sample preparation using $CE_{EXTRACTION}$ or $AE_{EXTRACTION}$ approaches.....3
Section 3. ESI-FT-ICR-MS tuning and quality control.....4
Section 4. Procedural Blanks.....6
Section 4. Assigned formulas of HA samples.....8
Section 6. Mass spectra of FA samples.....12
Section 7. Assigned formulas of FA samples.....13
Section 8. Application of $CE_{EXTRACTION}$ and SPE-PPL approaches on Suwannee River Fulvic Acid.....15
References.....18

Section 1. Sampling sites

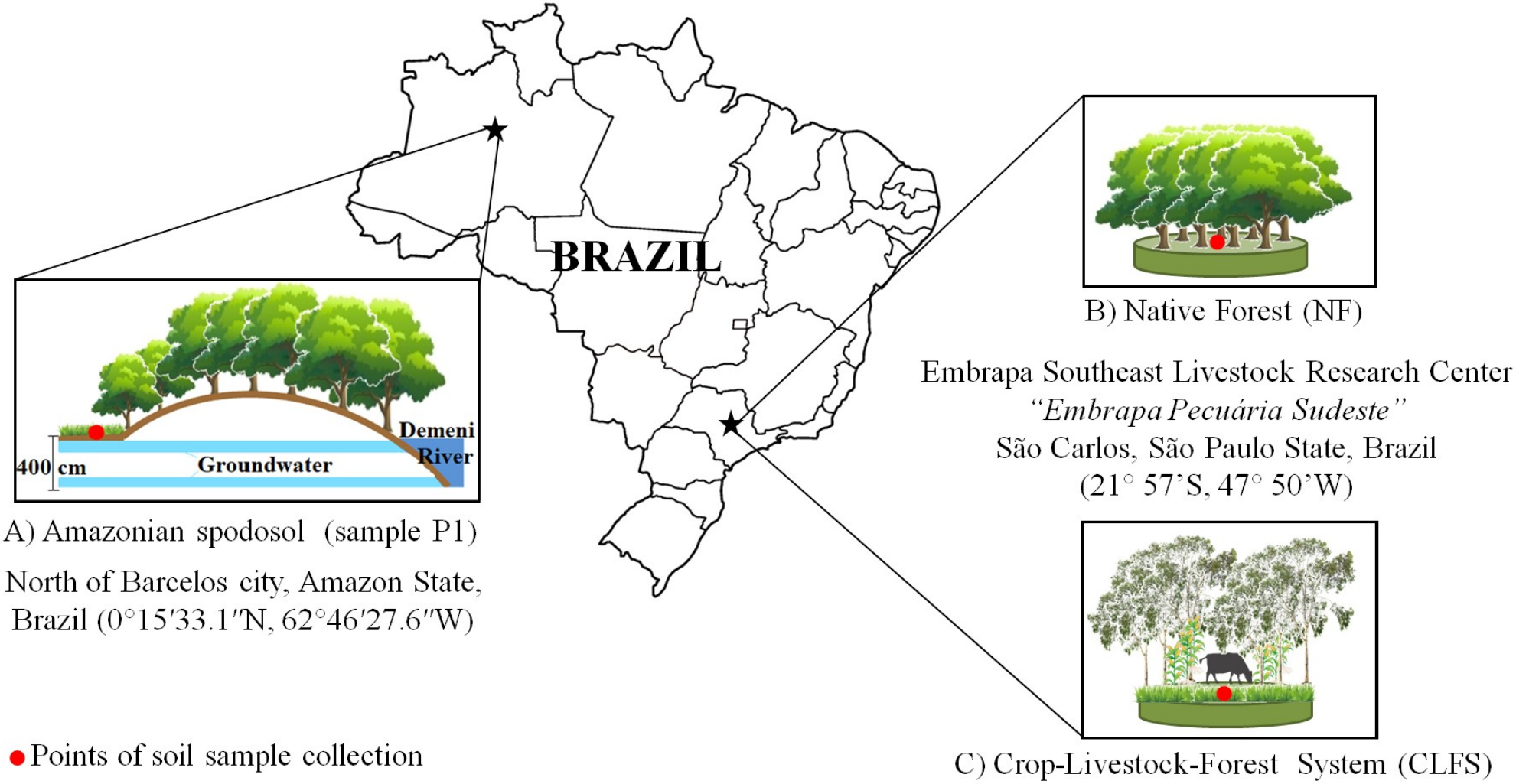

Figure S1: Illustration of different soil sample collection sites: A) Amazonian spodosol soils (sample P1), B) Atlantic Forest soil (sample Native Forest, NF); and C) agricultural study site (Crop-Livestock-Forest agricultural system, CLFS). Figures adapted from Tadini et al. (2018) and Tadini et al. (2021).

Section 2. Sample preparation using $CE_{EXTRACTION}$ approach

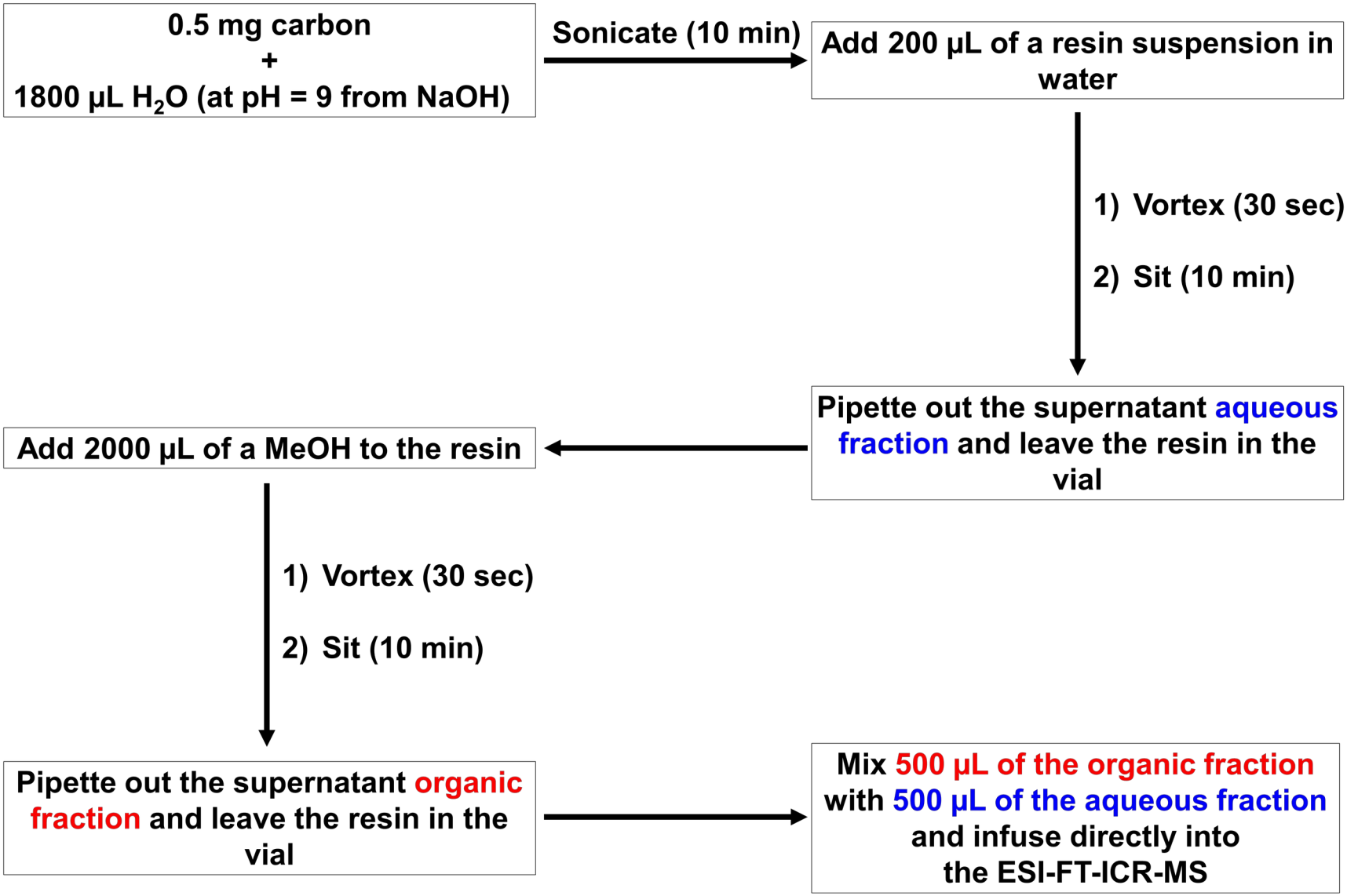

Figure S2. Flowchart for preparing samples using the $CE_{EXTRACTION}$ or $AE_{EXTRACTION}$ approaches.

Section 3. ESI-FT-ICR-MS tuning and quality control

The ESI-FT-ICR-MS mass spectrometer used in this study is calibrated daily with a freshly prepared polyethylene glycol (PEG) standard (Romson and Emmer, 2021) mixture. We use a 1:1 (w/w) mixture of PEG 400 (average molecular weight = 400 g/mol) and PEG 400 (average molecular weight = 600 g/mol) at a concentration of 1 µg/mL. Generally, only the elements of the transfer optics following after the second quadrupole are tuned, but other components are checked, and their parameters are tweaked if necessary. The transfer optics elements (accelerators, vertical and horizontal steers and focusing lenses) are critical for the formation of a tight ion packet that is to be transferred to the ICR cell. PEG is continuously infused into the source and parameters are altered in tuning mode until a spectrum of desirable mass range, gaussian shape and spectral magnitude (above 1 x 10^5) is achieved. Then, PEG is measured in acquisition mode with ion accumulation time in hexapole 1 of 0.05 s, ion accumulation time in hexapole 2 of 0.2 seconds, and 10 scans. It is then used to perform an external calibration across the mass range (typically m/z 300 – 800) as shown below.

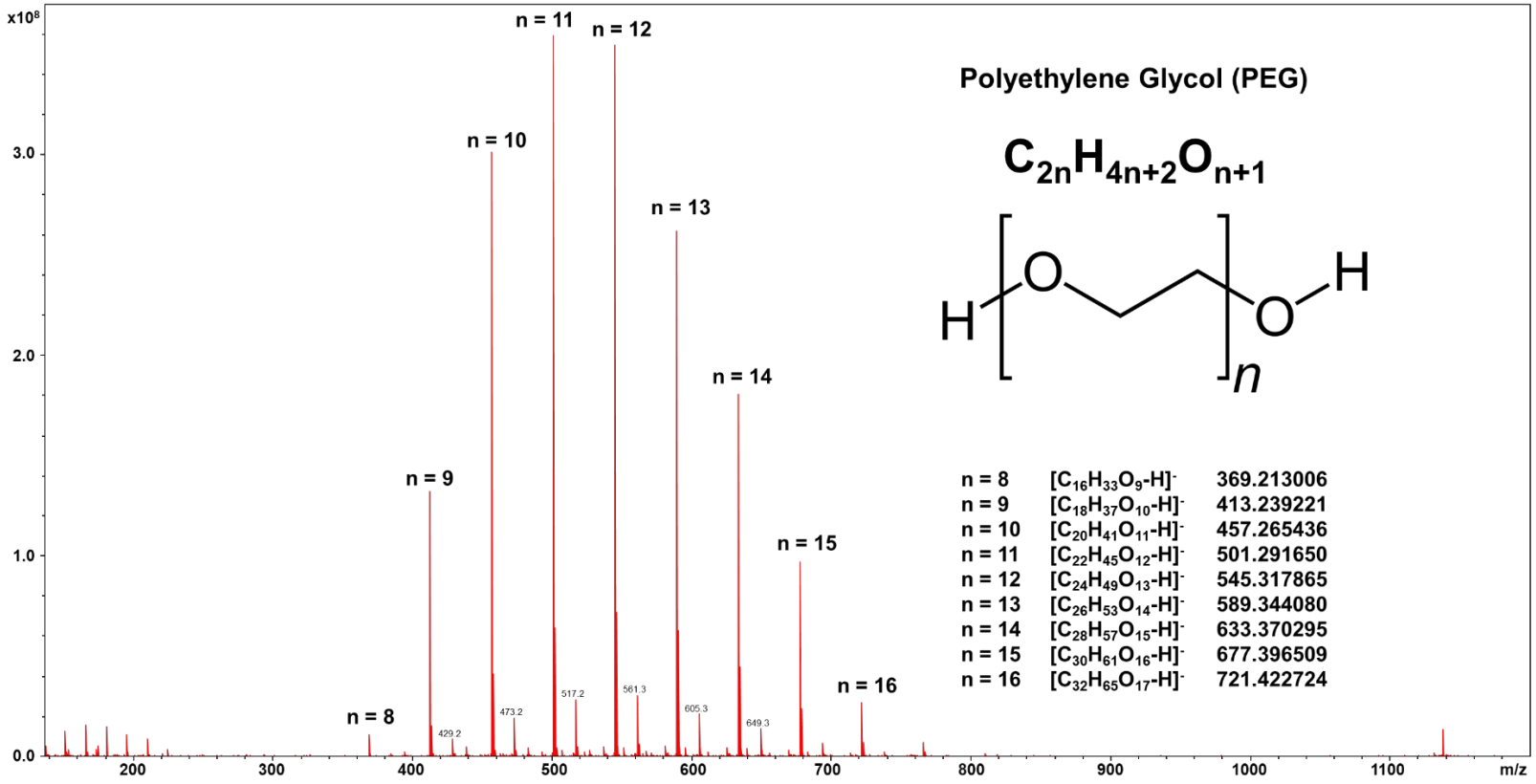

Figure S3. Polyethylene glycol (PEG) mass spectrum acquired in negative electrospray ionization mode.

Once external calibration is performed, Suwannee River fulvic acid (SRFA) standard from the International Humic Substances Society (https://humic-substances.org/) is used to validate the tuning following recommendations by the recent ESI-FT-ICR-MS interlaboratory comparison study (Hawkes et al., 2020). The powdered SRFA standard is dissolved as 40 mg/L carbon-equivalents in ultrapure laboratory-grade water (MilliQ). Then it is 2-fold diluted with methanol (Fisher Scientific, Optima LC-MS grade) to result in a 1:1 H_2O:MeOH mixture with 20 mg/L carbon-equivalents of SRFA. This solution is then immediately analyzed with ion accumulation time in hexapole 1 of 0.1 s, ion accumulation time in hexapole 2 of 0.5 seconds, and 300 scans. The obtained peak list is immediately internally calibrated and molecular formulas are assigned as described in the manuscript.

Section 4. Procedural blanks

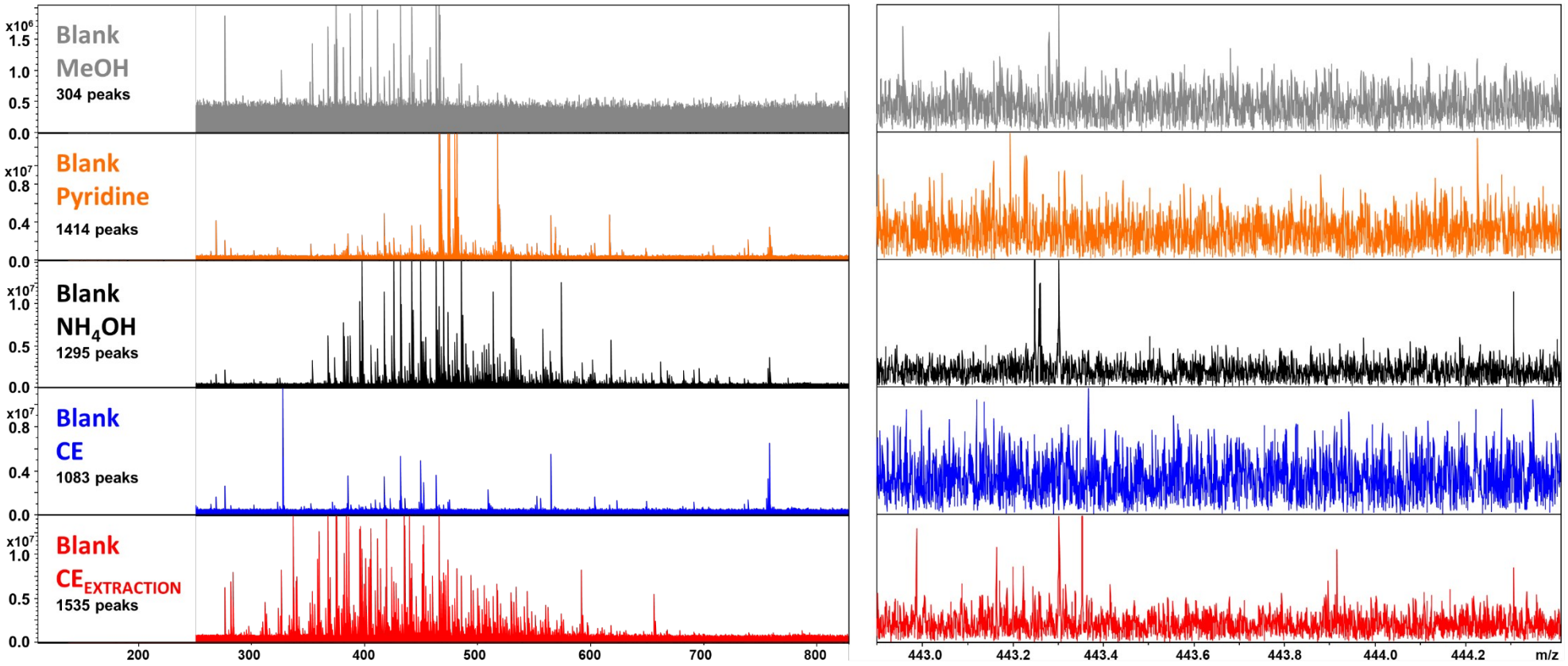

Figure S4: Whole ESI-FT-ICR-MS mass spectra (left) and expanded windows at nominal mass of 443 (right) for procedural blanks prepared using the five different solubilization approaches. Spectra are color coded as following: MeOH (**gray**), Pyridine (**orange**), NH_4OH (**black**), CE (**blue**), and $CE_{EXTRACTION}$ (**red**). Total number of detected peaks (S/N ≥ 3) is listed under the approach label.

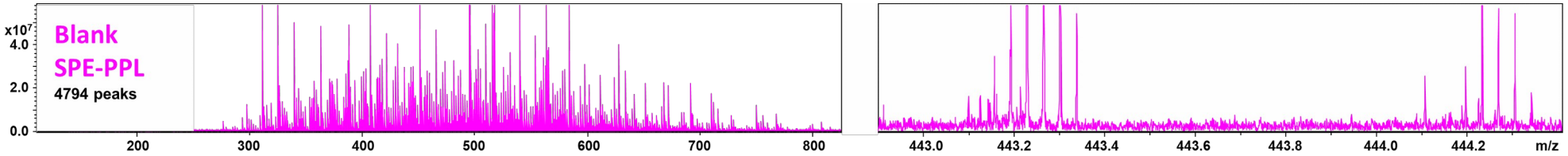

Figure S5. Whole ESI-FT-ICR-MS mass spectrum (left) and expanded window at nominal mass of 443 (right) for a procedural blank prepared using the SPE-PPL approach (**pink**). Total number of detected peaks (S/N ≥ 3) is listed under the approach label.

Section 4. Assigned formulas of soil HA samples

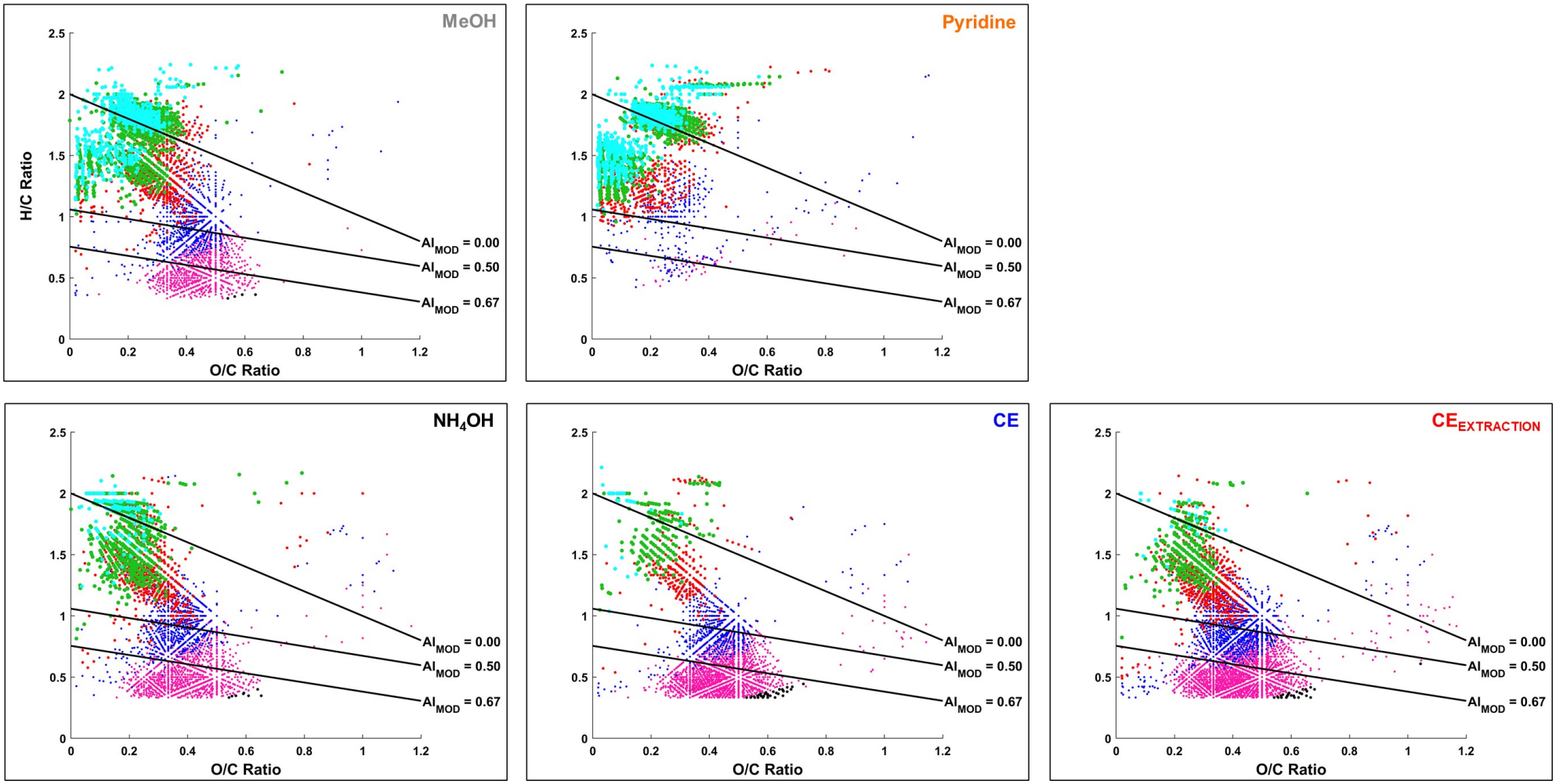

Figure S6. Van Krevelen diagrams (H/C vs O/C molar ratio plots) of assigned molecular formulas from a humic acid from a forest soil (native Atlantic Forest sample, NF) prepared using three different solubilization approaches: MeOH (**gray**), Pyridine (**orange**), NH_4OH (black), CE (**blue**), and $CE_{EXTRACTION}$ (**red**). Formulas are color coded based on mass defect of the observed molecular formulas: 0 – 0.1 in **pink**, 0.1 – 0.2 in **blue**, 0.2 – 0.3 in **red**, 0.3 – 0.4 in **green**, 0.4 – 0.7 in **cyan**, and 0.95 – 1 in **black**. The black lines indicate modified aromaticity index cutoffs (AI_{MOD})(Koch and Dittmar, 2006, 2016).

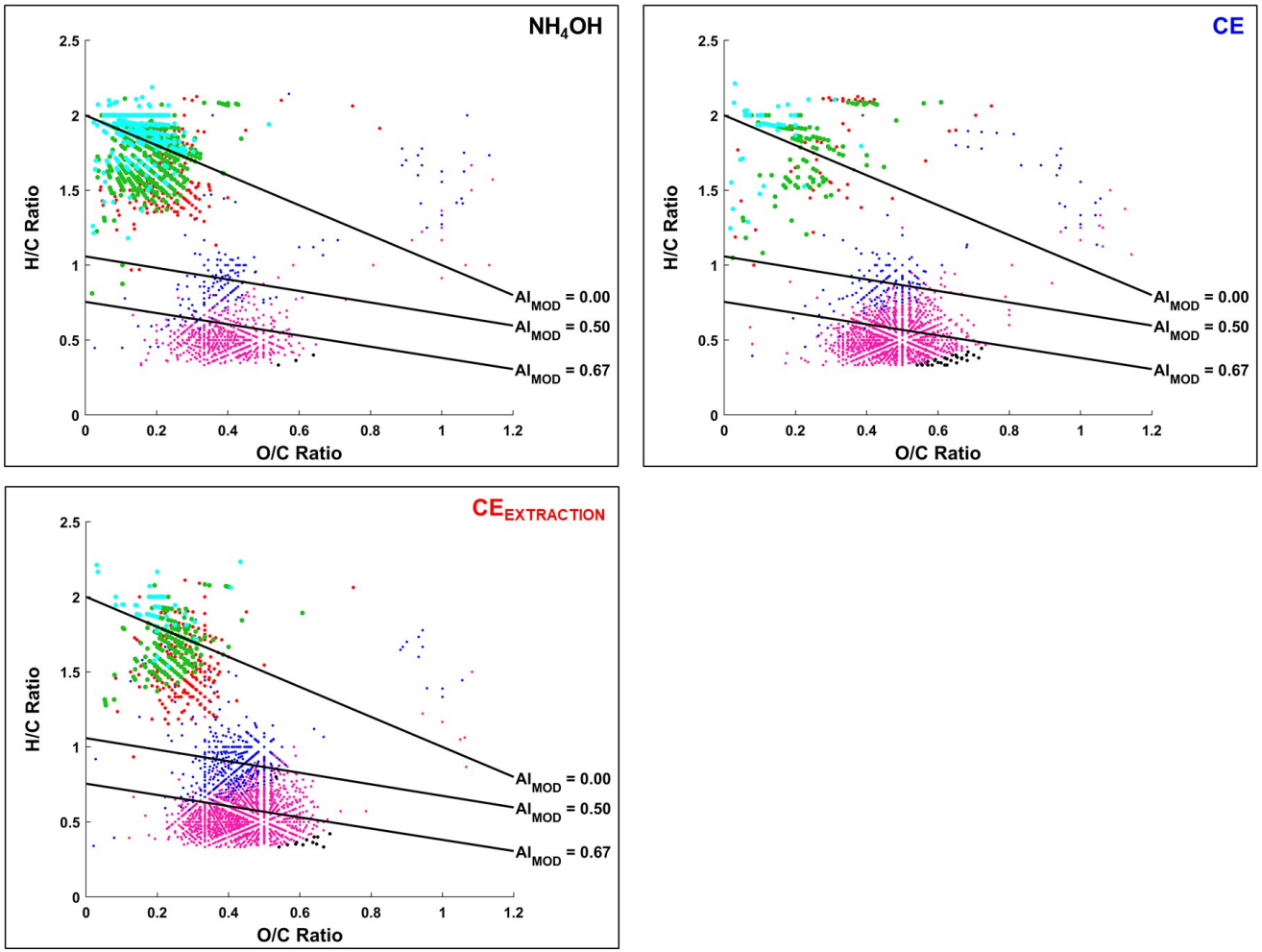

Figure S7: Van Krevelen diagrams (H/C vs O/C molar ratio plots) of assigned molecular formulas from a humic acid from a forest soil prepared using three different solubilization approaches: NH_4OH (black), CE (**blue**), and $CE_{EXTRACTION}$ (**red**). Formulas are color coded based on mass defect of the observed molecular formulas: 0 – 0.1 in pink, 0.1 – 0.2 in **blue**, 0.2 – 0.3 in **red**, 0.3 – 0.4 in **green**, 0.4 – 0.7 in **cyan**, and 0.95 – 1 in **black**. The black lines indicate modified aromaticity index cutoffs (AI_{MOD})(Koch and Dittmar, 2006, 2016).

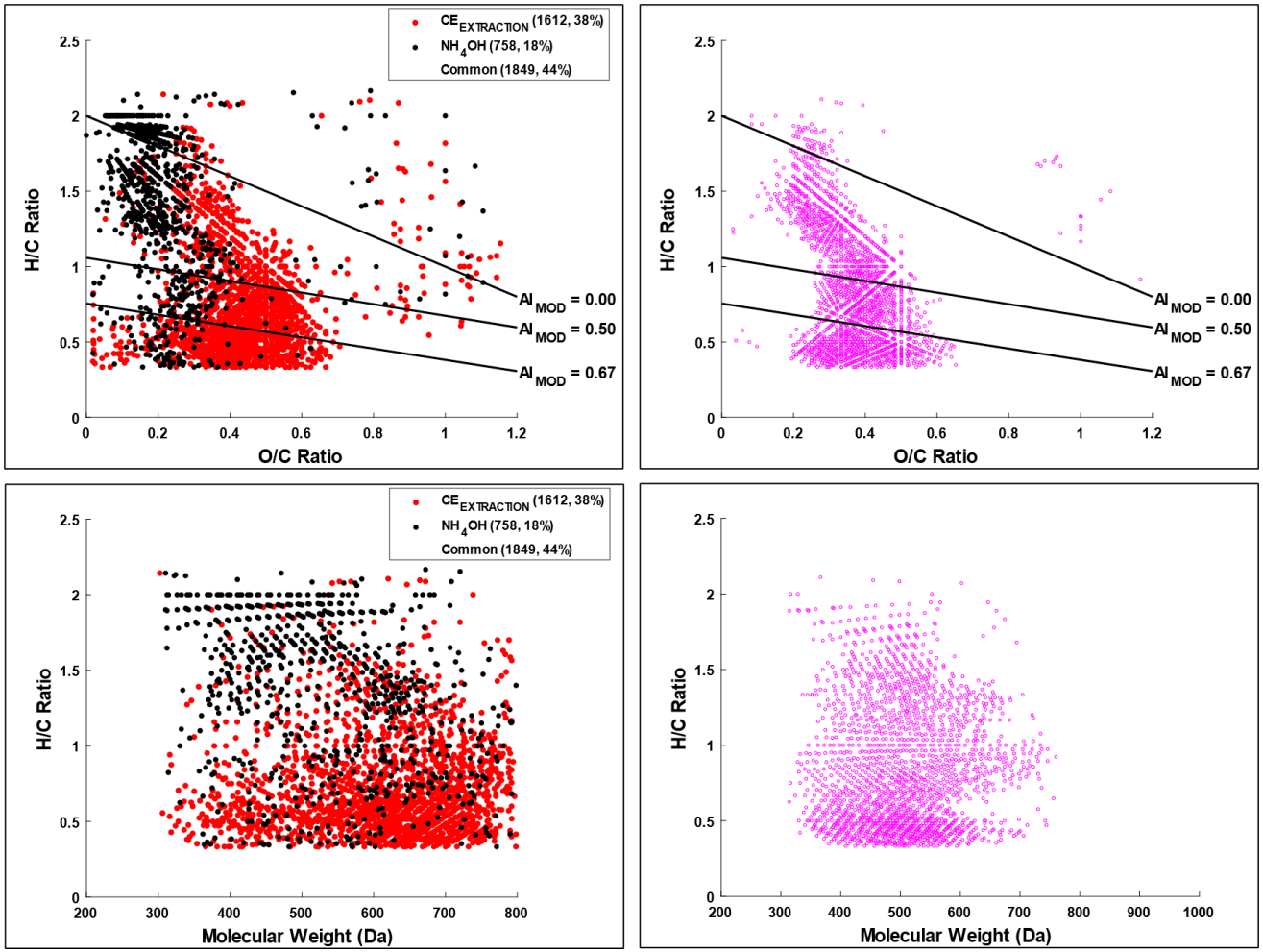

Figure S8: Van Krevelen diagrams (H/C vs O/C molar ratio plots) on top and H/C vs Molecular Weight plots on the bottom of assigned molecular formulas from a humic acid from a forest soil prepared using two different solubilization approaches: NH_4OH (**black**), and $CE_{EXTRACTION}$ (**red**). Formulas are assessed using presence/absence analysis (Sleighter et al., 2012) and formulas unique to the two samples are shown on the left panels while formulas common to both samples are shown on the right panels (in **pink**). The number of formulas found in each of these pools is listed in the legends along with corresponding percentages (relative to total number of formulas in the two samples being compared). The black lines on the van Krevelen diagrams indicate modified aromaticity index cutoffs (AI_{MOD})(Koch and Dittmar, 2006, 2016).

Section 5. ESI-FT-ICR-MS spectral multimodality of soil HA samples

Multimodal spectra have been previously observed (Blackburn et al., 2017; Cao et al., 2015) and it has been proposed that spectral multimodality is caused by instrument tuning (Cao et al., 2016), molecular aggregation from too concentrated samples (Fievre et al., 1997; Stenson et al., 2002) or molecular aggregation from using lower quality ESI sources (Kew et al., 2018). Spectra acquired on samples of low concentration of 2 – 50 mg-carbon/L (equivalent to 0.004 – 1.000 mg/mL organic matter assuming 50% carbon) do not aggregate (Kew et al., 2018; Witt et al., 2009). As the samples of this study are analyzed as 50 mg-carbon/L solutions, and the instrument was tuned following the recommendations by the recent ESI-FT-ICR-MS interlaboratory comparison study (Hawkes et al., 2020), the observed multimodality in the spectra for the MeOH and Pyridine approaches is likely not caused by instrument tuning or high sample concentration. The observed unimodal distributions of the rest of the samples (NH_4OH, CE, and $CE_{EXTRACTION}$) is indicative of the lack of aggregation when H_2O:MeOH solvent systems are used (Figure 1). The HA molecules in pyridine and methanol are likely of very different conformations due to the different solvent environment and thus solvent-induced aggregation must be considered (Joyce and Richards, 2011; Pape et al., 2014; Rodrigues et al., 2017). Modern instrument configurations and ion optics should break any ion aggregates that form (Kew et al., 2018), but our ESI-FT-ICR-MS is 10+ years old and it is possible that its ESI configuration was not capable of breaking any solvent-induced HA aggregates. Therefore, we conclude that the observed spectral multimodality following the MeOH and Pyridine approaches could be caused by aggregation. It is also possible that in MeOH or Pyridine environments, different molecular classes were ionized and suppressed causing the multimodal spectral shape. Lastly, it is possible that pyridine and methanol extracted different compound class molecules (as the HA samples were not completely solubilized) which caused the obtained liquid samples to be compositionally different. In conclusion, the observed differences in spectral shapes (Figure 1) are indicative that different solubilization approaches alter the analytical window of the technique and a sample preparation approach must be selected that provides the most representative molecular composition.

Section 6. Nitrogen-containing molecular formulas observed after MeOH and Pyridine approaches

The observation of many nitrogen-containing (1871 formulas, 88% of all) formulas in the CLFS sample when it was analyzed using the pyridine (Pyr) approach was intriguing and thus they were evaluated in greater detail. Out of these formulas, 738 were found in the MeOH sample and less than 10 were found in the NH_4OH, CE, or $CE_{EXTRACTION}$ samples. Thus, the N-containing molecules of the Pyridine sample could be artificially produced by coupling of pyridine with HA molecules via nitrogen incorporation into HA molecules (McKee et al., 2014). Upon closer examination, it was found that there were only 159 formulas existed in this sample that had an adduct formula ($C_{c+5}H_{h+5}N_{n+1}$) and a precursor formula ($C_cH_hN_n$) following chemical addition of pyridine (C_5H_5N). Thus, pyridine incorporation using Michael addition (McKee et al., 2014) was unlikely to have had occurred. It is possible that the majority of these N-containing molecules were preferentially extracted by pyridine from the HA as observed previously for aerosols (Willoughby et al., 2014). MeOH also exhibited an elevated N content (1404, 44% of all). Out of these formulas, 738 were found in the Pyridine sample and less than 160 were found in the NH_4OH, CE, or $CE_{EXTRACTION}$ samples. While MeOH cannot cause N-incorporation, it has been shown to preferentially extract N-containing molecules from soils (Tfaily et al., 2015). Thus, it is likely that Pyridine and MeOH preferentially extracted and/or enhanced the ionization of N-containing molecules rather than causing chemical incorporation of N into the HA molecules.

Section 7. Mass spectra of soil FA samples

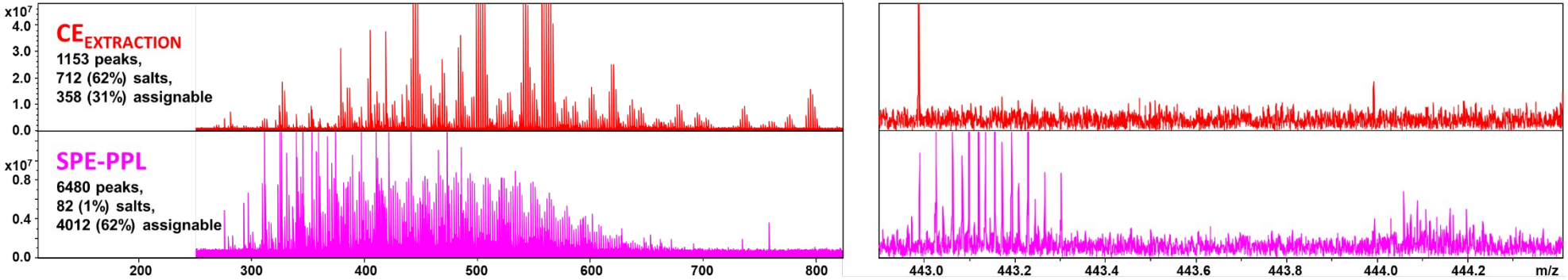

Figure S9: Whole ESI-FT-ICR-MS mass spectra (left) and expanded windows at nominal mass of 443 (right) a fulvic acid sample from a permanently waterlogged podzol soil (sample P1, horizon C) using two different solubilization approaches. Spectra are color coded as following: $CE_{EXTRACTION}$ (**red**), and SPE-PPL (**pink**). Statistics for each mass spectrum (total, salt, and assignable peaks) are listed under the approach label.

Section 8. Assigned formulas of soil FA samples

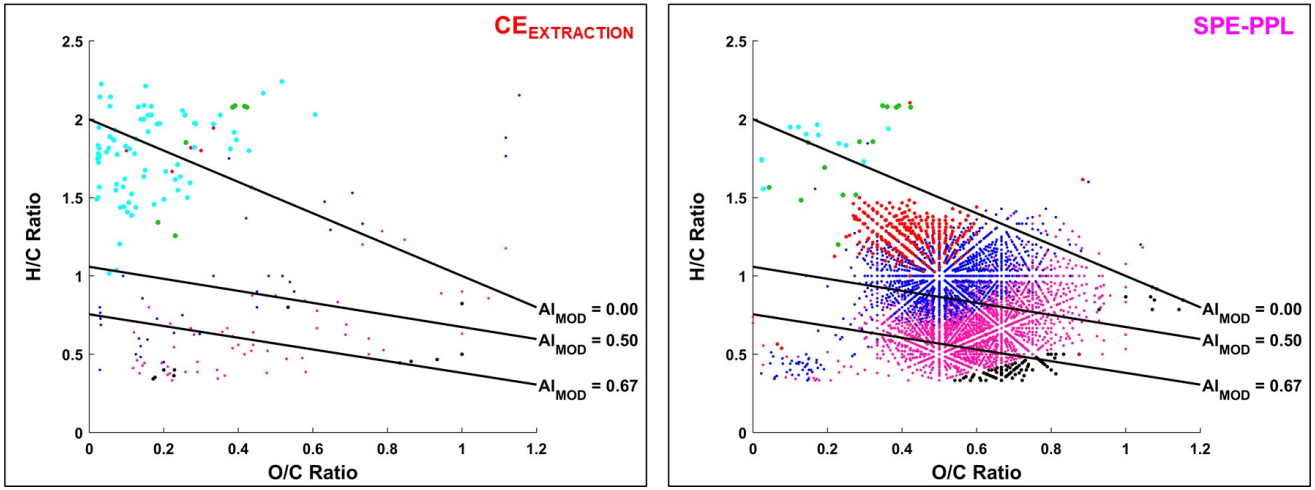

Figure S10. Van Krevelen diagrams (H/C vs O/C molar ratio plots) of assigned molecular formulas from a fulvic acid sample from a permanently waterlogged podzol soil (sample P1, horizon C) using two different solubilization approaches: $CE_{EXTRACTION}$ (**red**), and SPE-PPL (**pink**). Formulas are color coded based on mass defect of the observed molecular formulas: 0 – 0.1 in **pink**, 0.1 – 0.2 in **blue**, 0.2 – 0.3 in **red**, 0.3 – 0.4 in **green**, 0.4 – 0.7 in **cyan**, and 0.95 – 1 in **black**. The black lines indicate modified aromaticity index cutoffs (AI_{MOD})(Koch and Dittmar, 2006, 2016).

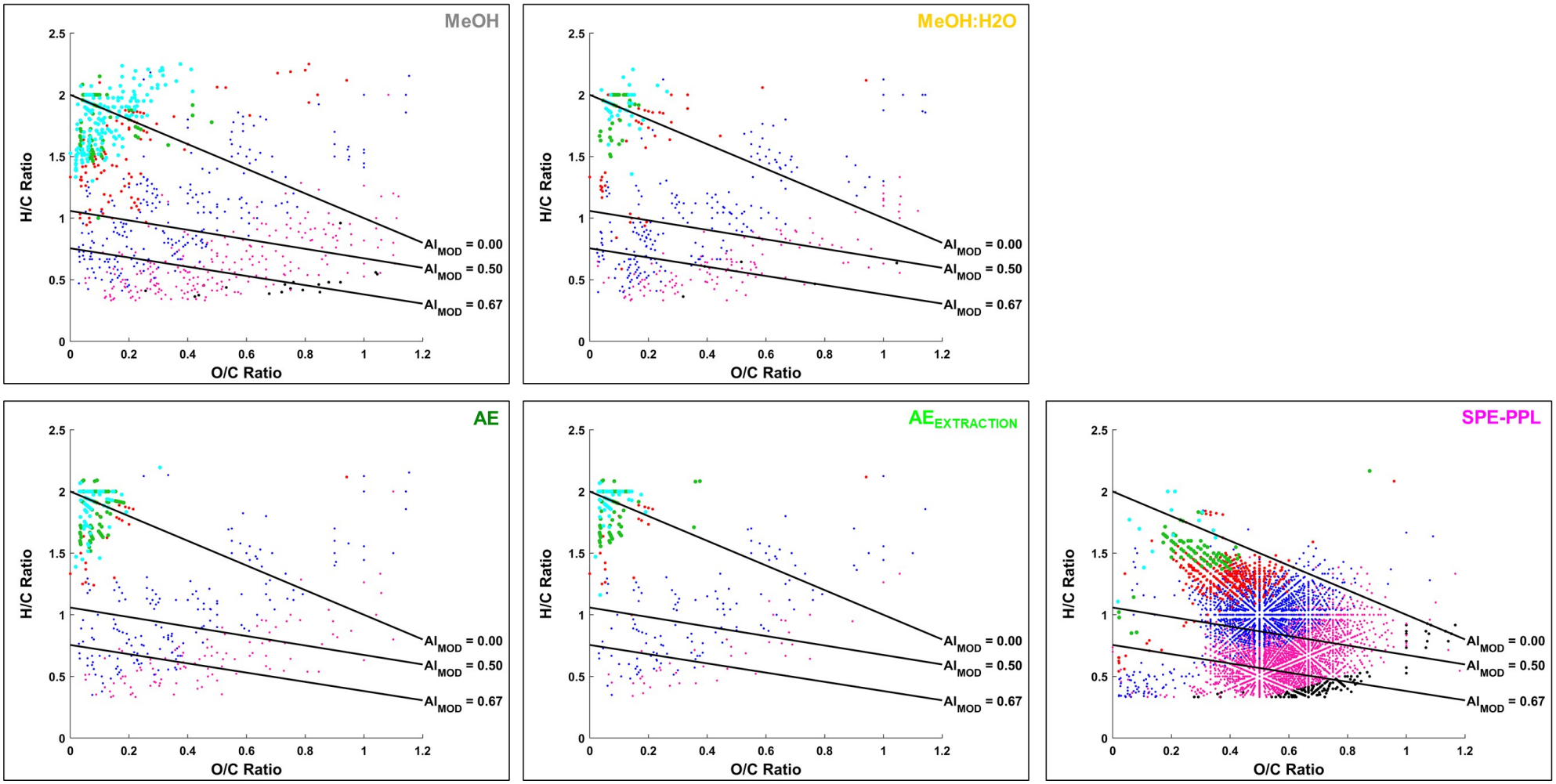

Figure S11. Van Krevelen diagrams (H/C vs O/C molar ratio plots) of assigned molecular formulas from a fulvic acid sample from a permanently waterlogged podzol soil (sample P1, horizon A) prepared using five different solubilization approaches: MeOH (**gray**), MeOH:H_2O (**yellow**), AE (**dark green**), $AE_{EXTRACTION}$ (**bright green**), and PPL (**purple**). Formulas are color coded based on mass defect of the observed molecular formulas: 0 – 0.1 in **pink**, 0.1 – 0.2 in **blue**, 0.2 – 0.3 in **red**, 0.3 – 0.4 in **green**, 0.4 – 0.7 in **cyan**, and 0.95 – 1 in **black**. The black lines indicate modified aromaticity index cutoffs (AI_{MOD})(Koch and Dittmar, 2006, 2016).

Section 8. Assigned formulas of Suwannee River FA samples

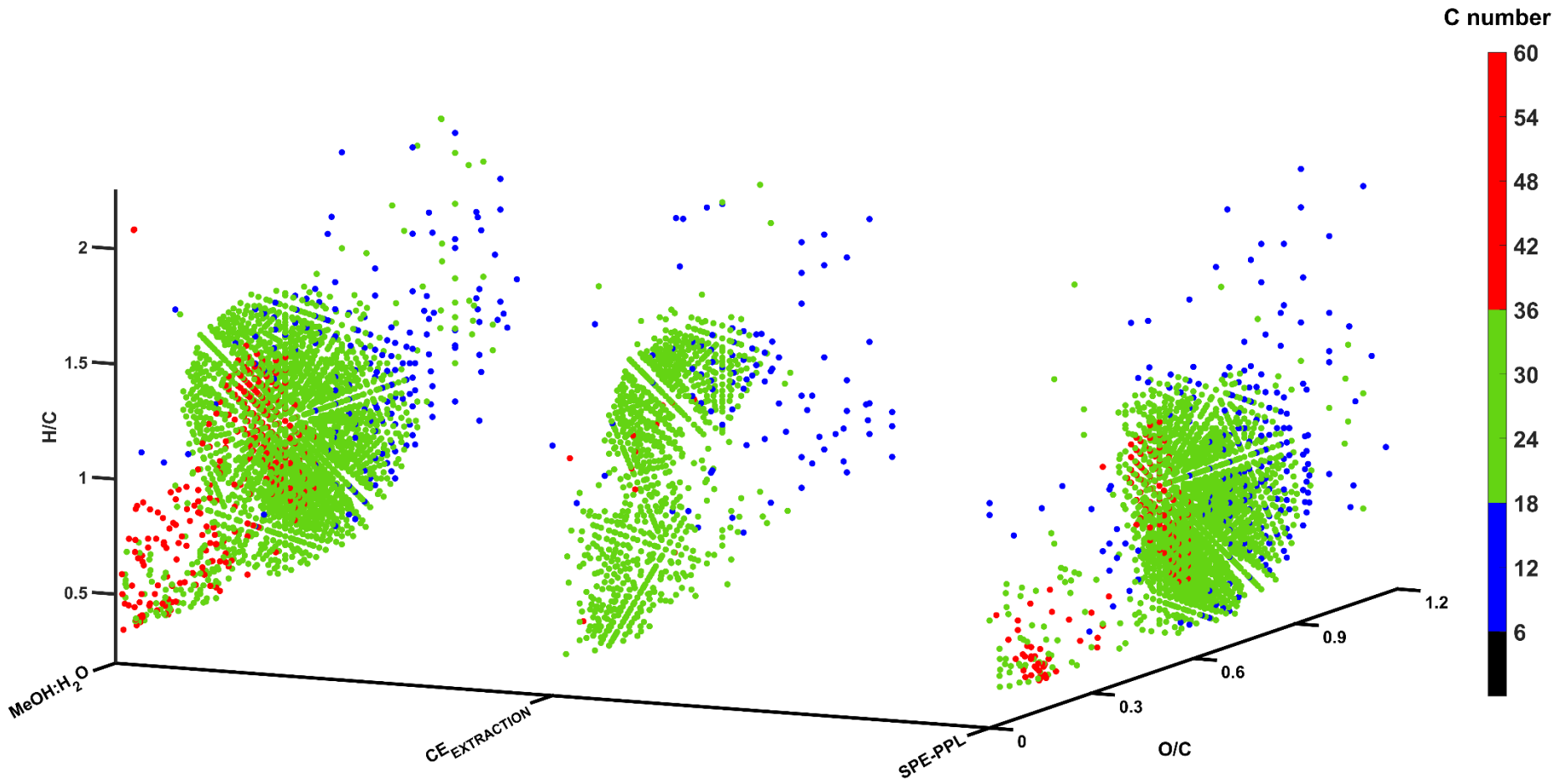

Figure S12. Van Krevelen diagrams of molecular formulas assigned to Suwannee River fulvic acid prepared using three different solubilization approaches: MeOH:H_2O (left), $CE_{EXTRACTION}$ (middle), SPE-PPL (right). Only formulas unique to one or two samples are shown. Common formulas to all three samples are shown on Figure S15.

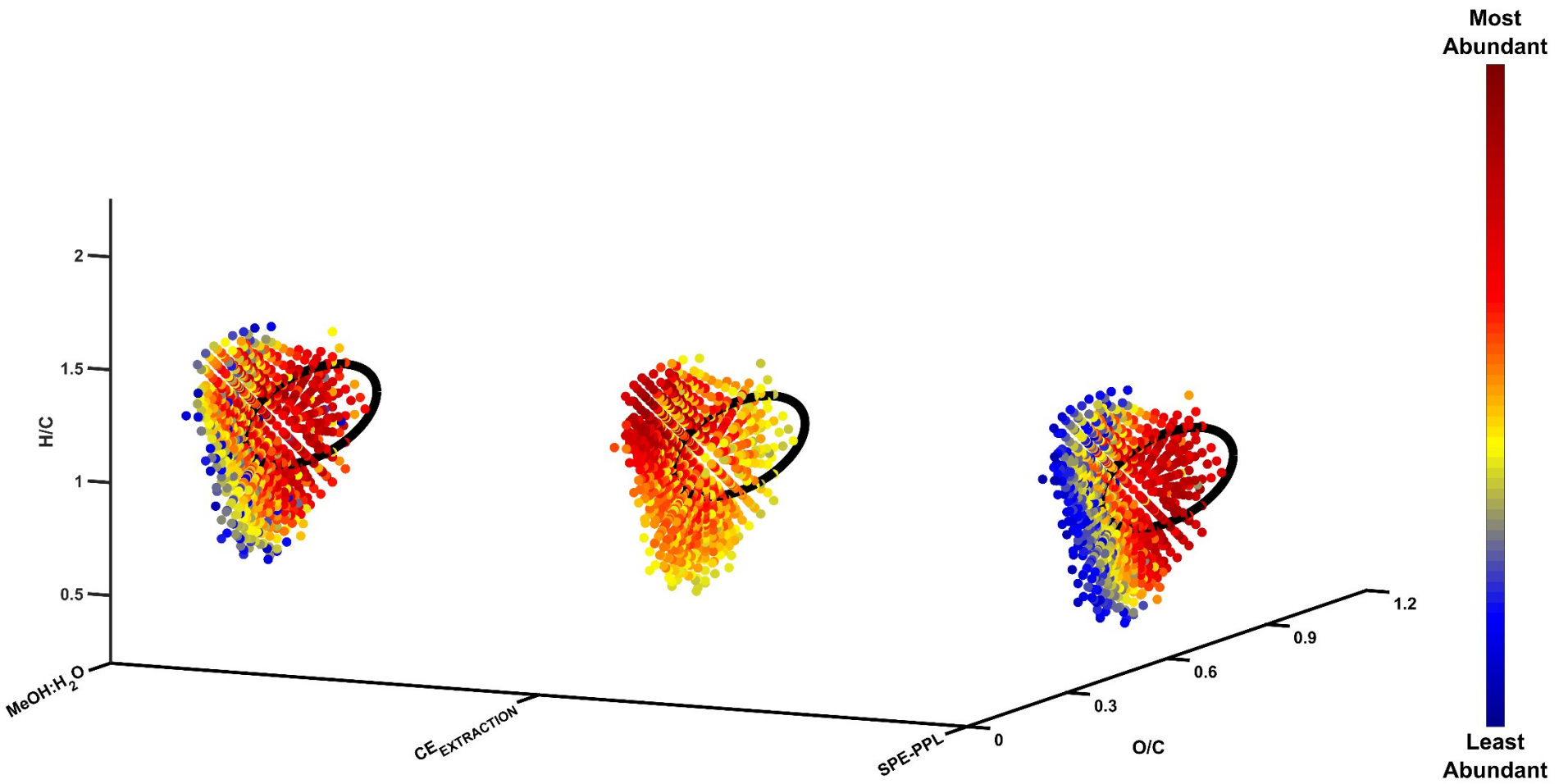

Figure S13. Van Krevelen diagrams of molecular formulas assigned to Suwannee River fulvic acid prepared using three different solubilization approaches: MeOH:H_2O (left), $CE_{EXTRACTION}$ (middle), SPE-PPL (right). Only common formulas to all three samples are shown.

References

Blackburn, J.W.T., Kew, W., Graham, M.C. and Uhrin, D. (2017) Laser Desorption/Ionization Coupled to FTICR Mass Spectrometry for Studies of Natural Organic Matter. Analytical Chemistry 89, 4382-4386.

Cao, D., Huang, H., Hu, M., Cui, L., Geng, F., Rao, Z., Niu, H., Cai, Y. and Kang, Y. (2015) Comprehensive characterization of natural organic matter by MALDI- and ESI-Fourier transform ion cyclotron resonance mass spectrometry. Analytica Chimica Acta 866, 48-58.

Cao, D., Lv, J., Geng, F., Rao, Z., Niu, H., Shi, Y., Cai, Y. and Kang, Y. (2016) Ion Accumulation Time Dependent Molecular Characterization of Natural Organic Matter Using Electrospray Ionization-Fourier Transform Ion Cyclotron Resonance Mass Spectrometry. Analytical Chemistry 88, 12210-12218.

Fievre, A., Solouki, T., Marshall, A.G. and Cooper, W.T. (1997) High-resolution Fourier transform ion cyclotron resonance mass spectrometry of humic and fulvic acids by laser desorption/ionization and electrospray ionization. Energy & Fuels 11, 554-560.

Hawkes, J.A., D'Andrilli, J., Agar, J.N., Barrow, M.P., Berg, S.M., Catalán, N., Chen, H., Chu, R.K., Cole, R.B., Dittmar, T., Gavard, R., Gleixner, G., Hatcher, P.G., He, C., Hess, N.J., Hutchins, R.H.S., Ijaz, A., Jones, H.E., Kew, W., Khaksari, M., Palacio Lozano, D.C., Lv, J., Mazzoleni, L.R., Noriega-Ortega, B.E., Osterholz, H., Radoman, N., Remucal, C.K., Schmitt, N.D., Schum, S.K., Shi, Q., Simon, C., Singer, G., Sleighter, R.L., Stubbins, A., Thomas, M.J., Tolic, N., Zhang, S., Zito, P. and Podgorski, D.C. (2020) An international laboratory comparison of dissolved organic matter composition by high resolution mass spectrometry: Are we getting the same answer? Limnology and Oceanography: Methods 18, 235-258.

Joyce, J.R. and Richards, D.S. (2011) Kinetic Control of Protonation in Electrospray Ionization. Journal of The American Society for Mass Spectrometry 22, 360-368.

Kew, W., Blackburn, J.W.T. and Uhrin, D. (2018) Response to Comment on "Laser Desorption/Ionization Coupled to FTICR Mass Spectrometry for Studies of Natural Organic Matter". Analytical Chemistry 90, 5968-5971.

Koch, B.P. and Dittmar, T. (2006) From mass to structure: An aromaticity index for high-resolution mass data of natural organic matter. Rapid Communications in Mass Spectrometry 20, 926-932.

Koch, B.P. and Dittmar, T. (2016) From mass to structure: An aromaticity index for high-resolution mass data of natural organic matter (Erratum). Rapid Communications in Mass Spectrometry 30, 1.

McKee, G.A., Kobiela, M.E. and Hatcher, P.G. (2014) Effect of Michael adduction on peptide preservation in natural waters. Environmental Science: Processes & Impacts 16, 2087-2097.

Pape, J., Vikse, K.L., Janusson, E., Taylor, N. and McIndoe, J.S. (2014) Solvent effects on surface activity of aggregate ions in electrospray ionization. International Journal of Mass Spectrometry 373, 66-71.

Rodrigues, M.A.A., Mendes, D.C., Ramamurthy, V. and Da Silva, J.P. (2017) ESI-MS of Cucurbituril Complexes Under Negative Polarity. Journal of The American Society for Mass Spectrometry 28, 2508-2514.

Romson, J. and Emmer, Å. (2021) Mass calibration options for accurate electrospray ionization mass spectrometry. International Journal of Mass Spectrometry 467, 116619.

Sleighter, R.L., Chen, H., Wozniak, A.S., Willoughby, A.S., Caricasole, P. and Hatcher, P.G. (2012) Establishing a measure of reproducibility of ultrahigh-resolution mass spectra for complex mixtures of natural organic matter. Analytical Chemistry 84, 9184-9191.

Stenson, A.C., Landing, W.M., Marshall, A.G. and Cooper, W.T. (2002) Ionization and fragmentation of humic substances in electrospray ionization Fourier transform-ion cyclotron resonance mass spectrometry. Analytical Chemistry 74, 4397-4409.
Tadini, A.M., Nicolodelli, G., Senesi, G.S., Ishida, D.A., Montes, C.R., Lucas, Y., Mounier, S., Guimarães, F.E.G. and Milori, D.M.B.P. (2018) Soil organic matter in podzol horizons of the Amazon region: Humification, recalcitrance, and dating. Science of The Total Environment 613-614, 160-167.
Tadini, A.M., Martin-Neto, L., Goranov, A.I., Milori, D.M.B.P., Bernardi, A.C.C., Oliveira, P.P.A., Pezzopane, J.R.M., Colnago, L.A. and Hatcher, P.G. (2021) Chemical characteristics of soil organic matter from integrated agricultural systems in southeastern Brazil. European Journal of Soil Science n/a, 1-18.
Tfaily, M.M., Chu, R.K., Tolić, N., Roscioli, K.M., Anderton, C.R., Paša-Tolić, L., Robinson, E.W. and Hess, N.J. (2015) Advanced Solvent Based Methods for Molecular Characterization of Soil Organic Matter by High-Resolution Mass Spectrometry. Analytical Chemistry 87, 5206-5215.
Willoughby, A.S., Wozniak, A.S. and Hatcher, P.G. (2014) A molecular-level approach for characterizing water-insoluble components of ambient organic aerosol particulates using ultrahigh-resolution mass spectrometry. Atmospheric Chemistry and Physics 14, 10299-10314.
Witt, M., Fuchser, J. and Koch, B.P. (2009) Fragmentation studies of fulvic acids using collision induced dissociation Fourier transform ion cyclotron resonance mass spectrometry. Analytical Chemistry 81, 2688-2694.